A Tunable Diode Based on an Inorganic Semiconductor | Conjugated Polymer Interface

Mark C. Lonergan

Although in principle semiconductor-metal (Schottky) diodes should be tunable by changing the work function of the metal, such flexibility cannot be achieved in a single device and in practice is often limited by interfacial states that cause Fermi-level pinning. A tunable diode is reported based on a hybrid inorganic-organic, *n*-indium phosphide | poly(pyrrole) | nonaqueous electrolyte architecture. By electrochemically manipulating the work function of the conjugated polymer poly(pyrrole), the turn-on voltage (more precisely, the forward bias potential required to pass a particular current) of the diode can be continuously and actively tuned by more than 0.6 volt. The work highlights a distinguishing feature of conjugated polymers relative to more traditional semiconductor materials, namely, the ability of dopant ions to permeate conjugated polymers, thereby enabling electrochemical manipulation.

The current-voltage (*I*-*V*) characteristics of an inorganic semiconductor (IS) | metal Schottky diode are largely determined by the potential barrier height ϕ_b at the interface. Small barrier heights yield ohmic contacts, and large barrier heights yield rectifying contacts that pass substantial current for one sign of the applied bias (forward bias) and negligible current for the other (reverse bias). In the ideal Schottky-Mott limit, the height of the potential barrier at Schottky diodes is given by (for an *n*-type semiconductor)

$$\phi_b = \phi_m - \chi \qquad (1a)$$

where ϕ_m is the metal work function and χ is the electron affinity of the semiconductor (*1*). Alternatively, one can write Eq. 1a in terms of the initial difference between the Fermi level of the metal $\mathbf{E}_{F,m}$ and the conduction band edge energy $\mathbf{E}_C$ of the *n*-type semiconductor

$$q\phi_b = \mathbf{E}_{F,m} - \mathbf{E}_C \qquad (1b)$$

where q is the elementary charge. With the vacuum level taken as zero, $\mathbf{E}_{F,m}$ (electron volts) is numerically equivalent to ϕ_m (volts), and $\mathbf{E}_C$ (electron volts) to χ (volts). The potential barrier at the interface is a consequence of the partial charge transfer that occurs upon contacting dissimilar materials. For *n*-type semiconductor | metal contacts, the more oxidizing the metal (larger ϕ_m), the greater this partial charge transfer, and consequently the larger ϕ_b (Fig. 1). A typical quantity used to characterize the forward-bias properties of a diode is the magnitude of the applied voltage $|V_F|$ required to pass a specified current I_F. For ideal Schottky junctions, $|V_F|$ increases linearly with ϕ_b (*1*, *2*). The Schottky-Mott limit, along with this relation between ϕ_b and $|V_F|$, suggests that the electrical properties of Schottky diodes based on a particular semiconductor can be systematically controlled through choice of metal. Experimentally, however, the level of control observed over ϕ_b is more limited than Eq. 1 would suggest. In many cases, ϕ_b is observed to be practically independent of metal, so-called Fermi-level pinning (*3*–*6*), with the degree of Fermi-level pinning given by an index of interface behavior, $S = d\phi_b/d\phi_m$. The ideal Schottky-Mott limit is given by $S = 1$ and the strongly Fermi-level pinned limit by $S = 0$. The breakdown of the simple Schottky-Mott relation is generally ascribed to interfacial layers (*7*, *8*), often a consequence of chemical reactions between the semiconductor and the metal, or to so-called metal-induced gap states (*9*). The presence of Fermi-level pinning can severely limit the flexibility of semiconductor-metal systems.

The use of a doped conjugated polymer (DCP) in place of a metal in Schottky-type diodes offers a number of potential advantages with regard to Fermi-level pinning (*10*). Two are highlighted here: (i) The macromolecular structure of the conjugated polymers implies the absence of surface dangling bonds, thereby minimizing the potential for interfacial reactions relative to metals (surface reconstruction and other processes due to dangling bonds on the surface of the inorganic semiconductor may, of course, still be problematic). (ii) The electrochemical potential of a single conjugated polymer can be tuned over a wide range while still preserving reasonable conductance (*11*). Much like ϕ_m is a measure of $\mathbf{E}_{F,m}$, the electrochemical potential E can be taken as a measure of the Fermi level of a conjugated polymer; and consequently for IS | DCP diodes, qE_{DCP} can essentially replace $\mathbf{E}_{F,m}$ in Eq. 1b, as long as all quantities are expressed on the same energy scale (*12*). The two points emphasized above suggest that extensive control over the electrical properties of an IS | DCP interface might be possible. Furthermore, unlike a metal, the E of a conjugated polymer can be actively controlled in an operational device by electrochemical means. In this report, the fabrication of a variable-barrier diode, based on the n-InP | poly(pyrrole) (PP) interface, is described that allows $|V_F|$ to be tuned continuously in a single device. By controlling the E of the PP (E_{PP}), $|V_F|$ can be controlled over a range greater than 0.6 V. Such control is much greater than that possible with n-InP | metal contacts and is achieved within the context of a single device rather than with a series of devices, each utilizing a different material.

The IS | DCP tunable diode studied (Fig. 2) consists of an n-InP | PP | gold minigrid sandwich with the gold grid side of the sandwich exposed to a nonaqueous electrolyte [0.1 M Bu_4NBF_4/CH_3CN (Bu = butyl)] (*13*). With the open minigrid, the conjugated polymer remains in contact with the electrolyte and can be electrochemically manipulated to set E_{PP}. Figure 3A shows a family of *I*-*V* curves collected for an n-InP | PP tunable diode. Each curve corresponds to a specific value of E_{PP} and exhibits the rectification behavior characteristic of a classic diode. By control of E_{PP}, the *I*-*V* traces can be shifted across the applied voltage axis. Over the range of E_{PP} shown in Fig. 3A, such shifts can be effected continuously and reversibly (*14*), with an increase

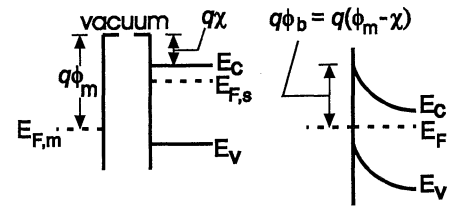

Fig. 1. Energy band diagrams for the formation of an ideal *n*-type semiconductor-metal interface (left, before contact; right, after contact). $\mathbf{E}_C$ and $\mathbf{E}_V$ are, respectively, the conduction and valence band edge energies of the *n*-type semiconductor; $\mathbf{E}_{F,m}$ and $\mathbf{E}_{F,s}$ are the Fermi levels of the metal and the semiconductor, respectively; ϕ_m is the metal work function; χ is the electron affinity of the semiconductor; and ϕ_b is the barrier height. Upon contacting the semiconductor and metal, partial charge transfer occurs to equilibrate their initially different Fermi levels. This charge transfer gives rise to a space charge region within the semiconductor and hence to an electric potential gradient, represented by the "bending" of the bands. The magnitude of the potential drop in the semiconductor is proportional to ϕ_b, which in turn is given by $\mathbf{E}_{F,m} - \mathbf{E}_C$ (Eq. 1). For an inorganic semiconductor | conjugated polymer interface, the picture is similar, with the Fermi level of the doped conjugated polymer replacing $\mathbf{E}_{F,m}$.

Department of Chemistry and the Materials Science Institute, University of Oregon, Eugene, OR 97403–1253, USA.

in the level of polymer oxidation (positive shift in E_{PP}) resulting in an increase in $|V_F|$. At $I_F = 1$ mA, $|V_F|$ is observed to shift by over 0.6 V in response to a 1.1-V change in E_{PP}. As shown in the inset to Fig. 3A, the increase in $|V_F|$ with E_{PP} is linear with $d|V_F|/dE_{PP} = 0.61 \pm 0.04$. If more extreme values of E_{PP} are considered than are shown in Fig. 3A, the system becomes irreversible for $E_{PP} > 1.1$ V versus the standard calomel electrode (SCE), presumably because the polymer overoxidizes or reacts with electrolyte impurities (or does both) (*15*); rectifying behavior is lost for E_{PP} somewhat more negative than the formal reduction potential of PP [$E^{o\prime}_{PP} = -0.1$ V versus SCE (*16*)] because the polymer is reduced to its insulating state. The *I-V* characteristics of a diode are generally well modeled by the diode equation (with the sign conventions as in Fig. 3A)

$$I = I_0\left[1 - \exp\left(-\frac{qV_{app}}{nk_BT}\right)\right] \qquad (2)$$

where I_0 is the equilibrium exchange current or reverse saturation current, n is the diode quality factor, V_{app} is the applied voltage, k_B is the Boltzmann constant, and T is the temperature (*17*, *18*). Both I_0 and n depend on the details of current flow at the interface, with the theoretical minimum of $n = 1$ generally considered ideal. For certain semiconductor diodes, multiple exponential behavior is observed in forward bias, indicating that different mechanisms of current flow (characterized by differing values of I_0 and n) dominate in different voltage ranges (*19*). Such behavior was observed for the n-InP|PP interface studied here (Fig. 3B). In particular for $E_{PP} < 0.66$ V versus SCE, two primary regions can be identified: (i) a region of lower applied voltage (termed region *L*) where the data converge to a common behavior characterized by the weakest dependence of *I* on *V* (highest quality factor, $n \approx 3$), and (ii) a region of higher applied voltage (termed region *H*) where the data are characterized by the strongest dependence of *I* on *V* (lowest quality factor, $n \approx 1.4$) and a dependence on E_{PP}. The applied voltage that separates regions *H* and *L* depends on E_{PP}, and in Fig. 3B the starting points of the solid-line fits roughly indicate the various dividing points between these regions. For $E_{PP} \geq 0.66$ V versus SCE, there is the hint of a third region of intermediate *n*, but given the quality and range of the data, it is difficult to distinguish this possibility from an *H* region with a somewhat higher quality factor ($n \approx 1.8$) than for $E_{PP} < 0.66$ V versus SCE (*20*).

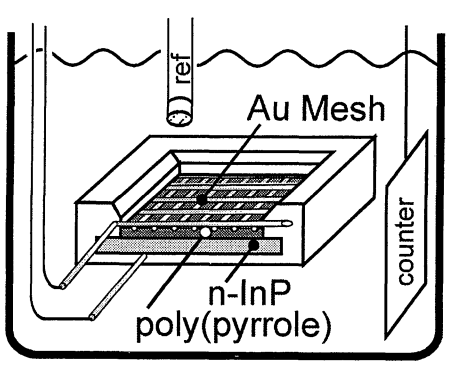

Fig. 2. Schematic of an n-InP|PP| nonaqueous electrolyte tunable diode [see text and (*13*) for further description].

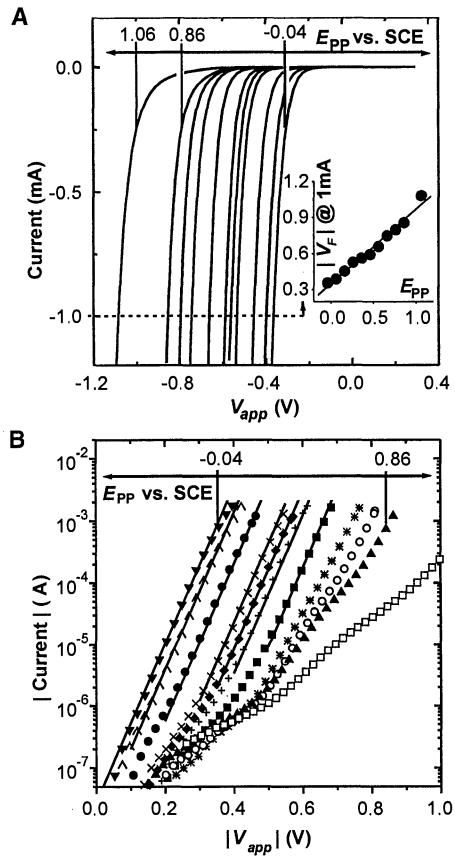

Fig 3. (**A**) *I-V* behavior of an n-InP|PP tunable diode as a function of the electrochemical potential of the PP E_{PP}. The far right trace is for $E_{PP} = -0.04$ V versus SCE, with the next nine traces to its left being a result of incremental 0.1-V positive shifts in E_{PP} up to 0.86 V versus SCE. The far left trace is for $E_{PP} = 1.06$ V versus SCE. Negative applied potentials correspond to higher electron energy in the n-InP relative to the PP, and negative currents correspond to net electron flow from the n-InP to the PP. The scan rate for these measurements was 50 mV s^{-1}. (**Inset**) The magnitude of the forward bias voltage $|V_F|$ required to pass 1 mA of current (the intercepts with the dotted line in the main plot) is shown as a function of E_{PP}. The solid line represents the result of a linear regression analysis that yielded $d|V_F|/dE_{PP} = 0.61 \pm 0.04$ and a correlation coefficient of $R = 0.98$. (**B**) Semilogarithmic representation of the forward bias data in (A) (note absolute values). The far left data set is for $E_{PP} = -0.04$ V versus SCE with the next nine sets to its right being a result of incremental 0.1-V positive shifts in E_{PP} up to 0.86 V versus SCE. The far right data set is for $E_{PP} = 1.06$ V versus SCE. The solid lines represent fits of the region *H* data (see text) to the diode equation with $n = 1.35$. For $E_{PP} \geq 0.66$ V, there is some ambiguity as to the definition of the *H* region (see text), and consequently these data are not fit.

Here we focus on region *H*, where there is a striking dependence on E_{PP} (best illustrated by the linear representation of Fig. 3A). This dependence can be understood by considering majority carrier electron transfer over the interfacial potential barrier in the absence of strong Fermi-level pinning. In this case, I_0 is given by

$$I_0 = aqk_nN_C\exp\left[\frac{-q\phi_b}{k_BT}\right] \qquad (3)$$

where *a* is the active device area, k_n is the surface recombination velocity, and N_C is the effective density of states (DOS) at the conduction band edge of the *n*-type inorganic semiconductor (*1*, *21*). From Eqs. 2 and 3 it can be seen that the forward bias current depends exponentially on both V_{app} and the potential barrier height ϕ_b. An increase in ϕ_b creates a larger barrier to current flow, and hence a larger forward bias voltage $|V_F|$ is required to pass a given current. In the absence of strong Fermi-level pinning, ϕ_b is expected to increase with a positive shift in E_{PP}, as described by Eq. 1b, for example, or by *S* more generally. Hence, a positive shift in E_{PP} is expected to result in an increase in ϕ_b and consequently an increase in $|V_F|$. Such behavior is observed at the n-InP|PP interface, where a positive shift in E_{PP} results in an increase in $|V_F|$ (Fig. 3A).

In the limit where k_n is independent of E_{PP}, the index of interface behavior can be calculated. It is given by $S = (1/n)d|V_F|/dE_{PP}$, and for the n-InP|PP interface studied here, $S = 0.44 \pm 0.03$ ($n = 1.4$; Fig. 3A inset). Although substantially less than the ideal value of $S = 1$, this value is still much better than observed at n-InP|metal contacts. Newman *et al.* measured ϕ_b for a series of n-InP|metal Schottky junctions and found the ϕ_b values to be pinned over a narrow 0.22-V range for nine metals covering a 1.05-eV range in ϕ_m (*5*). These values imply that $|V_F|$ can only be varied by 0.22 V, whereas the n-InP|PP interface allows $|V_F|$ to be varied by over 0.6 V for a similar change in *E*. Furthermore, little correlation was observed between ϕ_b and ϕ_m at the n-InP|metal interface. A linear regression of ϕ_b versus ϕ_m using the data of Newman *et al.* yielded a correlation coefficient of $R = 0.1$ and $S = 0.02$. In contrast, excellent correlation between $|V_F|$ and E_{PP}

is observed at the n-InP|poly(pyrrole) interface with $S = 0.44 \pm 0.03$ as mentioned earlier and $R = 0.98$ (Fig. 3A inset).

The much improved value of S suggests that interfacial reactions are either minimized or are less deleterious at the n-InP|PP interface relative to the n-InP|metal interface. Nonetheless, some density of interfacial defects may still be limiting S to less than 1. Perhaps a more intriguing possibility is that the nonideal behavior is due to a dependence of k_n on E_{PP}. Such a dependence implies that a change in barrier height with E_{PP} cannot be inferred directly from *I-V* measurements, because any observed shifts could in part be due to changes in k_n (Eq. 3). For intimate semiconductor-metal contacts, k_n is generally independent of metal and is given in the simplest case by Bethe's thermionic emission model for which $k_n = k_n^{TE} = (\bar{v}/4)$ where $\bar{v}$ is the average speed of electrons in the semiconductor (*1*, *22*). Although commonly applied to IS|DCP interfaces, there has been little direct experimental verification of Bethe's thermionic emission model as applied to Schottky-type diodes based on DCPs, and its validity has been questioned becaue of distinct differences in the DOS profiles of metals and DCPs (*23–25*). In particular, unlike k_n^{TE}, the surface recombination velocity at IS|DCP interfaces may depend on the DOS profile of the conjugated polymer at the band edge energy that is relevant for majority carrier transfer (*24*), in much the same way as observed for certain semiconductor|liquid redox couple contacts (*21*).

The electrical properties of IS|DCP interfaces as a function of E_{DCP} have been reported by other workers, but for the interfaces studied thus far, *I-V* properties were largely independent of E_{DCP}. Watanabe *et al.* have measured the electrical properties of press-contacted n-Si|PP interfaces as a function of E_{PP} (*26*). Here the only effects observed were due to changes in the bulk resistance of the PP. Such an observation is not surprising in light of other measurements on n-Si|PP interfaces with $E_{PP} \approx 0.3$ V versus SCE. These measurements demonstrate that a dependence on ϕ_b and hence E_{PP} is not necessarily expected because current flow, at least for $E_{PP} = 0.3$ V versus SCE, is not dominated by majority carrier electron transfer over the interfacial potential barrier. Rather, minority carrier bulk recombination (no dependence on ϕ_b expected) dominates (*27*). Frank *et al.* have measured the electrical characteristics of n-CdS|PMeT [PMeT = poly(3-methyl thiophene)] interfaces while exposing the conjugated polymer to aqueous solutions of redox couples of varying electrochemical potentials (*28*). Such a procedure essentially results in E_{PMeT} equilibrating to that of the redox electrolyte to which it is contacted. Although the presence of the redox couple somewhat complicates interpretation, variation of the E of the redox couple and hence of E_{PMeT} did not result in any substantial or systematic change in the electrical properties of the buried n-CdS|PMeT interface. The presence of Fermi-level pinning in this later case was argued to be due to surface states caused by corrosion reactions. Such reactions are minimized in our work in part through the choice of material, in particular the use of a nonaqueous electrolyte (*29*, *30*).

The tunable diode presented represents a new type of device architecture that, unlike more traditional architectures, can exploit the electrochemical control over E that is possible with conjugated polymers. The approach extends and combines into a single device the range of effective barrier heights accessible with semiconductor diodes based on n-InP. Furthermore, it provides a general route to diodes with specific properties for specialized applications. Beyond its novel device properties, the IS|DCP|electrolyte configuration provides an excellent platform for studying the mechanisms of Fermi-level pinning and for probing the details of electron transfer at semiconductor interfaces. It is a special platform for such studies in that the Fermi level of the semiconductor contact can be varied with the use of a single interface rather than a series of interfaces fabricated from different materials.

REFERENCES AND NOTES

1. E. H. Rhoderick and R. H. Williams, *Metal-Semiconductor Contacts*, P. Hammond and R. L. Grimsdale, Eds. (Monographs in Electrical and Electronic Engineering, Oxford Univ. Press, Oxford, ed. 2, 1988), vol. 19.
2. For $q|V_F| > 3$ kT.
3. M. J. Turner and E. H. Rhoderick, *Solid State Electron.* **11**, 291 (1968).
4. H. Jager and W. Kosak, *ibid.* **12**, 511 (1969).
5. N. Newman, T. Kendelewicz, L. Bowman, W. E. Spicer, *Appl. Phys. Lett.* **46**, 1176 (1985).
6. N. Newman, W. E. Spicer, T. Kendelewicz, I. Lindau, *J. Vac. Sci. Technol. B* **4**, 931 (1986).
7. J. Bardeen, *Phys. Rev.* **71**, 717 (1947).
8. W. E. Spicer, I. Lindau, P. Skeath, C. Y. Su, P. W. Chye, *Phys. Rev. Lett.* **44**, 420 (1980).
9. V. Heine, *Phys. Rev. A* **138**, 1689 (1965).
10. The use of the term "Schottky-type" refers to the belief that a substantial depletion width only exists in the inorganic semiconductor, as with semiconductor-metal Schottky diodes. Such behavior is expected because the dopant atoms within intentionally doped PP are mobile and therefore unable to support a space charge region as in inorganic semiconductors. Experimental evidence for this comes from preliminary capacitance-voltage measurements and from the fact that n-InP|PP interfaces fabricated with highly doped (degenerate) n-InP yield ohmic contacts, which indicates that there is not a substantial depletion width in the doped conjugated polymer. These studies have only been carried out with the as-synthesized PP ($E_{PP} \approx 0.3$ V versus SCE), and consequently the possibility of a depletion region in the conjugated polymer influencing interfacial charge transfer cannot be ruled out for all values of E_{PP}. In particular, at very low doping levels (likely much lower than those studied here), depletion can be supported by a small density of immobile intrinsic defect states.
11. D. Ofer, R. M. Crooks, M. S. Wrighton, *J. Am. Chem. Soc.* **112**, 7869 (1990).
12. H. Reiss and A. Heller, *J. Phys. Chem.* **89**, 4207 (1985).
13. To fabricate the n-InP|PP| minigrid sandwich, a piece of single-crystal n-InP (orientation 100, carrier density $\approx 1 \times 10^{16}$ cm^{-3}, 350 μm thick; Crystacomm, Mountain View, CA), ohmically back-contacted with Ga/In eutectic, was first imbedded ≈50 μm below the flat surface of an epoxy encasement. A gold minigrid (60-μm wire diameter, 250-μm spacing, 65% open; Goodfellow, Berwyn, PA) was then suspended above the n-InP with its edges ohmically contacted and embedded in epoxy. The n-InP electrode was doubly etched (each etch consisted of the following sequence: 30 s in 0.05% Br_2/MeOH, MeOH rinse, 30 s in 30% $NH_4OH_{(aq)}$, water rinse) and immediately transferred to a dry N_2 environment. All subsequent manipulations were carried out under dry N_2. PP with an as-synthesized conductivity of 10 to 20 ohm^{-1} cm^{-1} was deposited from solution through the gold grid by means of the method of Freund *et al.* (*16*) to a thickness sufficient to span the gold grid and the n-InP. The resulting structure was placed into an electrochemical cell filled with 0.10 M tetrabutylammonium tetrafluoroborate (Bu_4NBF_4, dried for a minimum of 7 days in vacuum at 80°C; Johnson Matthey, Ward Hill, MA) in acetonitrile (CH_3CN, distilled under N_2 from CaH_2 then P_2O_5; Mallinckrodt, Phillipsburg, NJ). The electrochemical cell was fitted with a nonaqueous Ag/$AgNO_3$ (≈0.005 M in 0.10 M Bu_4NBF_4/CH_3CN) reference electrode and a Pt counter electrode separated off with a porous glass frit. E_{PP} was controlled versus the Ag/$AgNO_3$ reference with a Solartron 1287 potentiostat/galvanostat and a three-electrode configuration (gold grid, working electrode; Pt flag, counter electrode; Ag/$AgNO_3$, reference electrode). E_{PP} was appropriately converted and is reported relative to aqueous SCE. The Solartron 1287 was also used for *I-V* measurements across the n-InP|PP interface, with the leads being switched to an appropriate two-electrode configuration (n-InP, "working" electrode; gold grid, "counter/reference" electrode).
14. Although extensive studies of stability and reversibility have yet to be conducted, an n-InP|PP interface in the course of being switched repeatedly among 10 different values of E_{PP} has been brought through $E_{PP} = 0.06$ V versus SCE five times with good overlap of the *I-V* curves. With the current geometry, switching times are relatively long and of course depend on the values of E_{PP} one desires to switch between. In general, a 0.1-V shift in E_{PP} requires on the order of 5 min with our device geometry and potentiostatic control. To ensure equilibrium in the data of Fig. 3, the PP layer was driven to the desired E_{PP} for two sequental 10- to 20-min periods; the *I-V* curves collected after the first and second periods were in good agreement, indicating that equilibrium was achieved after the first.
15. At these more oxidizing potentials, substantial drift in both the *I-V* characteristics and E_{PP} was also noted. For instance, in one experiment a polymer driven to $E_{PP} = 1.3$ V versus SCE for 20 min drifted to $E_{PP} = 1.1$ V versus SCE within 10 min of removal of potentiostatic control.
16. M. S. Freund, C. Karp, N. S. Lewis, *Curr. Sep.* **13**, 66 (1994).
17. Unlike Eq. 2, a more rigorous form of the diode equation accounts for the action of the quality factor on the reverse bias data [see (*1*)].
18. S. M. Sze, *Physics of Semiconductor Devices* (Wiley, New York, 1981).
19. A. Y. C. Yu and E. H. Snow, *J. Appl. Phys.* **39**, 3008 (1968).
20. The upper current limit that is accessible is limited by series resistance effects. The downward curvatures of the highest current data for $E_{PP} = -0.04$ and 0.06 V versus SCE in Fig. 3B are in fact due to series resistance effects.
21. N. S. Lewis, *Annu. Rev. Phys. Chem.* **42**, 543 (1991).

22. H. A. Bethe, *Theory of the Boundary Layer of Crystal Rectifiers* (Radiation Laboratory, Massachusetts Institute of Technology, Cambridge, MA 1942).
23. Evidence for the failure of thermionic emission to describe current flow at IS|DCP junctions can be seen from the disagreement observed by several workers between barrier heights determined from capacitance-voltage measurements and from *I-V* measurements using thermionic emission theory. See, for example, (*25*) and (*28*).
24. A. Kumar, W. C. A. Wilisch, N. S. Lewis, *Crit. Rev. Solid State Mater.* **18**, 327 (1993).
25. M. Ozaki *et al.*, *Appl. Phys. Lett.* **35**, 83 (1979).
26. A. Watanabe, S. Murakami, K. Mori, Y. Kashiwaba, *Macromolecules* **22**, 4231 (1989).
27. M. C. Lonergan, J. Yamamoto, N. S. Lewis, in preparation.
28. A. J. Frank, S. Glenis, A. J. Nelson, *J. Phys. Chem.* **93**, 3818 (1989).
29. M. J. Heben, C. Kumar, C. Zheng, N. S. Lewis, *Nature* **340**, 621 (1989).
30. The stability of n-InP in nonaqueous solvents has been demonstrated in the context of n-InP photoelectrochemical cells. See, for example (*29*).
31. Supported by the University of Oregon, the Dreyfus Foundation, and NSF (Career, DMR-9703311). I thank J. E. Hutchison, J. D. Cohen, N. S. Lewis, J. A. Myers, and C. T. Cooney for helpful discussions.

15 August 1997; accepted 4 November 1997

Estimating the Mass of Asteroid 253 Mathilde from Tracking Data During the NEAR Flyby

D. K. Yeomans,* J.-P. Barriot, D. W. Dunham, R. W. Farquhar, J. D. Giorgini, C. E. Helfrich, A. S. Konopliv, J. V. McAdams, J. K. Miller, W. M. Owen Jr., D. J. Scheeres,† S. P. Synnott, B. G. Williams

The terminal navigation of the Near Earth Asteroid Rendezvous (NEAR) spacecraft during its close flyby of asteroid 253 Mathilde involved coordinated efforts to determine the heliocentric orbits of the spacecraft and Mathilde and then to determine the relative trajectory of the spacecraft with respect to Mathilde. The gravitational perturbation of Mathilde on the passing spacecraft was apparent in the spacecraft tracking data. As a result of the accurate targeting achieved, these data could be used to determine Mathilde's mass as 1.033 ($\pm$ 0.044) $\times$ 10^{20} grams. Coupled with a volume estimate provided by the NEAR imaging team, this mass suggests a low bulk density for Mathilde of 1.3 grams per cubic centimeter.

The NEAR spacecraft was designed to rendezvous with asteroid 433 Eros in January 1999 and spend 13 months in close orbit about this near-Earth object. As such, the design and instrumentation of the NEAR spacecraft were optimized for the close orbit of Eros. While refining the trajectory required to effect an Eros rendezvous, the NEAR project identified an opportunity to fly past the unusual and relatively large asteroid 253 Mathilde on 27 June 1997. Although the Galileo spacecraft had made successful flybys of asteroids 951 Gaspra and 243 Ida in 1991 and 1993, both of these asteroids were relatively bright and of the spectral class termed S, whereas Mathilde was thought to be black and of spectral class C (*1*). In addition, the relatively large size of Mathilde and the close flyby distance of 1212 km provided an opportunity to determine Mathilde's mass.

Accurate navigation of the NEAR spacecraft's flyby of Mathilde was required if any of the science objectives were to be realized (*2*). The NEAR spacecraft flew past Mathilde at about 10 km s^{-1}, close to the planned flyby distance of 1200 km. The flyby distance was selected as a trade-off between a distance that was close enough to provide high-resolution (160 m per pixel) images at closest approach, yet far enough so that the angular slew rate would not be too high and there would be enough time for slewing the spacecraft and camera to image the entire area of the sky within which Mathilde was expected. The imaging sequence onboard the NEAR spacecraft could tolerate an error of about 20 s in the time of closest approach before the closest encounter images would be lost. A major source for the NEAR spacecraft's targeting error was the uncertainty in the predicted position of Mathilde (ephemeris uncertainty) at the time of encounter, and this could be improved using approach optical navigation imaging data (hereafter called OpNavs) taken onboard the spacecraft. The final ground-based pre-encounter orbit of Mathilde (JPL reference orbit 49) was based on 610 position observations from 5 December 1885 through 24 June 1997 (*3*).

For fast flybys of target bodies, position errors are often expressed in the so-called "impact plane" of the spacecraft. This impact plane coordinate system is defined by the unitized relative velocity vector between the spacecraft and asteroid at closest approach (**S**), a unit vector (**T**) that is parallel to the Earth mean equator (J2000) and normal to **S**, and by the unit vector $\mathbf{R} = \mathbf{S} \times \mathbf{T}$. The vector **R** points south and **T** points west. Vectors **R** and **T** define the impact plane at closest approach, whereas vector **S** is directed along the relative velocity vector and perpendicular to the impact plane. By using the optical navigation images of the asteroid as seen by the spacecraft (described below), a best estimate of the asteroid's actual position in space at the time of the encounter was determined. The consistency of the results as more and more ground-based pre-encounter observations were included in orbital solutions, as well as the very small differences between the observed and predicted positions of Mathilde (generally less than 0.05 arc sec), allowed an accurate mid-course maneuver to be performed 9 days before the encounter. As a result, a risky maneuver at encounter minus 12 hours was canceled. On the basis of ground-based pre-encounter astrometry alone, the actual Mathilde ephemeris error was only 9 km in the **T** direction and 27 km in the **R** direction. The corresponding error in the direction of the spacecraft's relative velocity was 12.6 km, or, expressed in terms of the time-of-flight error, 1.3 s. (All errors and uncertainties are 1σ values throughout this report.) From ground-based observations alone, the error of Mathilde's ephemeris, at the time of encounter, was less than the size of the asteroid itself.

In addition to providing accurate positional information for Mathilde using Earth-based observations alone, it was necessary to refine these positions with Mathilde images (OpNavs) taken onboard the spacecraft itself. The NEAR flight team took a total of 96 OpNavs of Mathilde against a star background during the last 2 days before the flyby. Because Mathilde was only 40° from the sun, the spacecraft had to be turned so that the solar panels pointed 50° from the sun. The resulting loss of power made these maneuvers risky, and it was decided to take pictures at only six different times, beginning at 41 hours be-

D. K. Yeomans, J. D. Giorgini, C. E. Helfrich, A. S. Konopliv, J. K. Miller, W. M. Owen Jr., D. J. Scheeres, S. P. Synnott, B. G. Williams, Navigation and Flight Mechanics Section, Jet Propulsion Laboratory (JPL), California Institute of Technology, Pasadena, CA 91109, USA.
J.-P. Barriot, Department of Terrestrial and Planetary Geodesy, Centre National d'Etudes Spatiales, Toulouse, France.
D. W. Dunham, R. W. Farquhar, J. V. McAdams, Applied Physics Laboratory, Johns Hopkins University, Laurel, MD 20723, USA.

*To whom correspondence should be addressed. E-mail: donald.k.yeomans@jpl.nasa.gov
†Present address: Department of Aerospace Engineering and Engineering Mechanics, Iowa State University, Ames, IA 50011, USA.